

York, 1952), Chap. 9, Sec. 21.

¹⁶G. N. Watson, *A Treatise on the Theory of Bessel Functions* (Cambridge U. P., Cambridge, England, 1966), 2nd ed., Chap. 9.

¹⁷Reference 16, Chap. 5, Sec. 21 or Chap. 16.

¹⁸H. Cramer, *Mathematical Methods of Statistics* (Princeton U. P., Princeton, N. J., 1945), pp. 222–223. The author is indebted to B. Gravely and F. Lado for this reference. This expansion also has been used by R. Bersohn and T. P. Das, *Phys. Rev.* **130**, 98 (1963).

¹⁹*Handbook of Mathematical Functions*, edited by M. Abramowitz and I. A. Stegun (Dover, New York, 1965), p. 485.

²⁰D. E. O'Reilly and T. Tsang, *Phys. Rev.* **128**, 2639 (1962).

²¹D. E. Barnaal and I. J. Lowe, *Phys. Rev.* **148**, 328 (1966).

²²G. Glebashev, *Zh Eksperim. i Teor. Fiz.* **32**, 82 (1957) [*Soviet Phys. JETP* **5**, 38 (1957)].

²³E. R. Andrew, *Phys. Rev.* **91**, 425 (1953).

PHYSICAL REVIEW B

VOLUME 2, NUMBER 7

1 OCTOBER 1970

Antiresonance in the Optical Spectra of Transition-Metal Ions in Crystals*

M. D. Sturge[†] and H. J. Guggenheim

Bell Telephone Laboratories, Murray Hill, New Jersey 07974

and

M. H. L. Pryce

Department of Physics, University of British Columbia, Vancouver 8, British Columbia

(Received 8 May 1970)

When a sharp absorption line of a defect or impurity center is overlapped by a broad vibronic band, interference can occur between the two types of transition. We find several examples of this effect in the optical spectrum of V^{2+} in octahedral fluoride coordination. The spectral line shapes can be fitted well by the four-parameter theory of Fano, which was developed to account for the interference of a sharp intra-atomic transition with an overlapping ionizing continuum. We justify the application of this theory to the vibronic problem, and calculate some of the parameters in terms of other spectroscopic data, obtaining good agreement with experiment.

I. INTRODUCTION

Among the more remarkable features of the spectra of the rare gases are the Beutler bands.^{1,2} These occur when sharp intra-atomic transitions are overlapped by a broad ionizing continuum. The transition matrix elements interfere destructively on one side of the intra-atomic resonance and constructively on the other, giving a characteristic "antiresonant" spectral line shape. A particularly elegant example is to be seen in the hard ultraviolet absorption spectrum of HeI^3 ; the $1s^2 \rightarrow 2s$, np series looks like a series of dispersion curves superimposed on the continuum of ionizing transitions which leave the He^+ ion in the $1s$ state. Similar effects are to be expected in the predissociation region of molecular spectra.⁴

The theory of this effect has been given by Fano.⁵ The formalism is identical to that of the Breit-Wigner⁶ theory of scattering from resonant nuclei. Fano shows that if the continuum absorption $\alpha_B(\omega)$ is slowly varying in the vicinity of an isolated resonance, the absorption coefficient $\alpha(\omega)$ is given by

$$\alpha(\omega) = \alpha_B(\omega) + \alpha_0(q^2 + 2\xi q - 1)/(1 + \xi^2), \quad (1)$$

where

$$\xi = (\omega - \omega_r)/\gamma, \quad q = \frac{\langle s' | \vec{P} | a \rangle}{\pi \langle s | \mathcal{H} | c \rangle \langle c | \vec{P} | a \rangle},$$

$$\frac{\alpha_0}{\alpha_B} = \frac{|\langle c | \vec{P} | a \rangle|^2}{|\langle b | \vec{P} | a \rangle|^2} \equiv p, \quad \gamma = \pi |\langle c | \mathcal{H} | s \rangle|^2.$$

Here $|s\rangle$ is the sharp excited state; $|s'\rangle$ is that state modified by the interaction Hamiltonian \mathcal{H}_i , which connects $|s\rangle$ to a certain fraction $|c\rangle$ of the continuum states $|b\rangle$. The energy of $|s'\rangle$ above the ground state $|a\rangle$ is $\hbar\omega_r$, and γ^{-1} can be interpreted as the lifetime of the sharp state against decay to the continuum. \vec{P} is the electric- or magnetic-dipole operator. The quantity q may take any value between $-\infty$ and $+\infty$, and $q^2\gamma$ is a measure of the strength of transitions to the modified sharp state $|s'\rangle$, relative to the continuum $|c\rangle$.

Equation (1) can be represented by a family of curves corresponding to different values of q , as shown, normalized by a factor $(1 + q^2)^{-1}$, in Fig. 1.

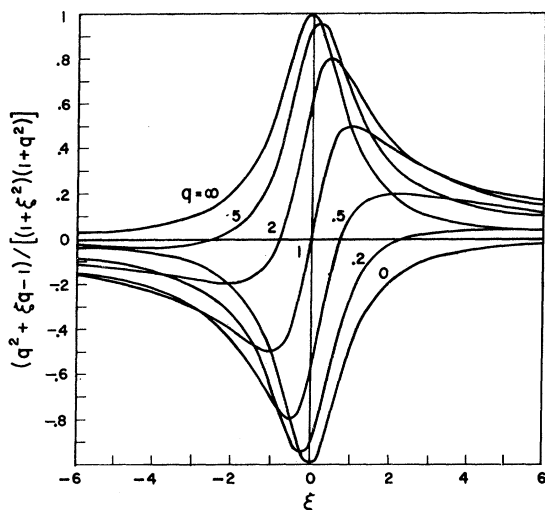


FIG. 1. Equation (1) divided by $(1 + q^2)$, with $\alpha_0 = 1$, and a variety of positive values for q . For negative q , the figure should be inverted about the axis $\xi = 0$.

The spectral line shape ranges from the normal Lorentzian resonance for $|q| = \infty$, through a dispersionlike curve for $|q| = 1$, to an inverted Lorentzian (antiresonance) for $q = 0$.

Features resembling the Beutler bands, though usually less pronounced, have been found in the absorption spectra of solids. Excitonic transitions overlapped by band-to-band continua show asymmetries which can be attributed to interference.⁷⁻⁹ Sharp transitions of impurity centers sometimes interfere with band-to-band transitions of the host crystal.^{10,11} The theory of the latter effect has been studied by Toyozawa and his associates,¹¹ but the experimental data obtained up till now are too complex to be compared quantitatively with his calculations.

In all these cases there is a close analogy with the atomic case considered by Fano, since the final continuum states are those of a "free" conduction electron. However, interference is sometimes observed in cases where the final state is a vibrational continuum. For instance, interference between first-order Raman lines and the continuum of second-order scattering occurs in BaTiO_3 .¹² Analogous effects have been seen in the infrared reflectivity of this and other highly polarizable perovskites,¹³ and in x-ray and neutron scattering from alkali halides.¹⁴ Complicated absorption spectra showing the asymmetric peaks and dips characteristic of interference effects are seen in large aromatic molecules, where sharp Rydberg transitions overlap vibrationally broadened $\pi \rightarrow \pi^*$ transitions.¹⁵ Finally, in certain favorable cases, well-resolved antiresonances are found in the absorption spectra

of transition-metal impurities in solids.¹⁶ We discuss these in detail below.

The Fano theory has been applied to the latter class of problems, but its applicability cannot be taken for granted. There is a great difference between a multiphonon continuum, with many degrees of freedom, and the continuum of states of a single free electron, which has only three. It is the primary purpose of this paper to develop a theory of interference in the spectra of transition-metal ions which not only justifies the use of Fano's formula (1) but makes quantitative predictions of the parameters in it.

We discuss in Sec. II several antiresonances in the absorption spectrum of the $(3d)^3$ ion V^{2+} , incorporated as a dilute impurity into KMgF_3 and MgF_2 , including a more detailed account of results briefly reported earlier.¹⁶ Interference occurs between sharp transitions within the t_2^3 configuration, which are either phononless or involve the emission of one phonon of relatively well-defined energy, and broad transitions in which several phonons are emitted. The latter are spin allowed; the former are spin forbidden because of the Pauli principle, but are made allowed by spin-orbit coupling to the overlapping spin-allowed band. The spectra can be fitted by (1), and a set of parameters is obtained which it is the concern of our theory to explain.

In Sec. III, we set up a model for an impurity ion in a solid which we believe represents the physical situation for V^{2+} in KMgF_3 reasonably accurately. We show that this model leads to Eq. (1), plus some additional terms which we prove to be small. In Sec. IV, we apply the theory to the problem in hand, and calculate values for the parameters q and γ which are in good agreement with experiment.

II. EXPERIMENT

Single crystals of KMgF_3 , doped with approximately 0.3% V^{2+} , were grown by the method described elsewhere.¹⁷ We measured their absorption spectra at temperatures down to 2°K on a Cary 14RI double-beam spectrophotometer fitted with a cooled RCA 7102 photomultiplier. The resolution was 2 to 3 cm^{-1} . To eliminate the possibility that fluorescence was distorting the spectrum, we compared the absorption spectra obtained with the specimen in the entrance and in the exit optics of the spectrometer. They were identical. Furthermore, we searched unsuccessfully for fluorescence in the relevant spectral regions, using an argon-ion laser as the exciting source.

The over-all optical spectrum of V^{2+} in KMgF_3 is described and interpreted elsewhere.^{17,18} The main features with which we are concerned are illustrated by the schematic energy-level diagram shown in Fig. 2. There are two strong absorption bands,

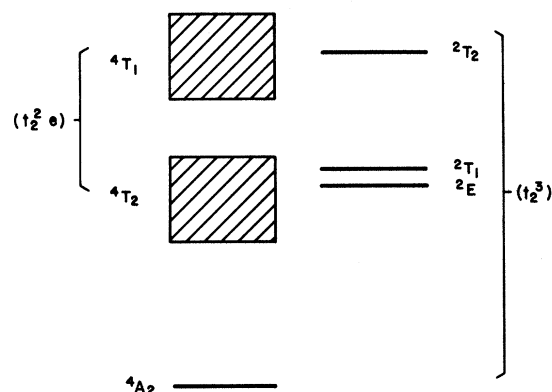


FIG. 2. Lower energy levels of V^{2+} in octahedral F^- coordination (schematic). Spin-orbit coupling and noncubic fields are neglected.

some 2000 cm^{-1} wide, with maxima at $12\,150$ and $18\,400\text{ cm}^{-1}$. These are spin-allowed transitions from the 4A_2 ground term to the 4T_2 and 4T_1 excited terms of the d^3 configuration, and involve the raising of an electron from a t_2 to an e orbital. There are also weak, but relatively sharp, spin-forbidden transitions to the 2E , 2T_1 , and 2T_2 terms, at $12\,675$, $13\,350$, and $18\,430\text{ cm}^{-1}$. (The 2T_1 state is split by spin-orbit coupling into Γ_8 and Γ_6 levels, 35 cm^{-1} apart.) These transitions involve no change of orbital. They are overlapped by the broad bands, and the absorption spectrum in their vicinity is shown in Figs. 3 and 4.

The bands can be fitted, away from the sharp transitions, by the "Pekarian" form^{19,20}

$$\alpha_B = \alpha_0 e^{-S} p^S / \Gamma(p+1), \quad (2)$$

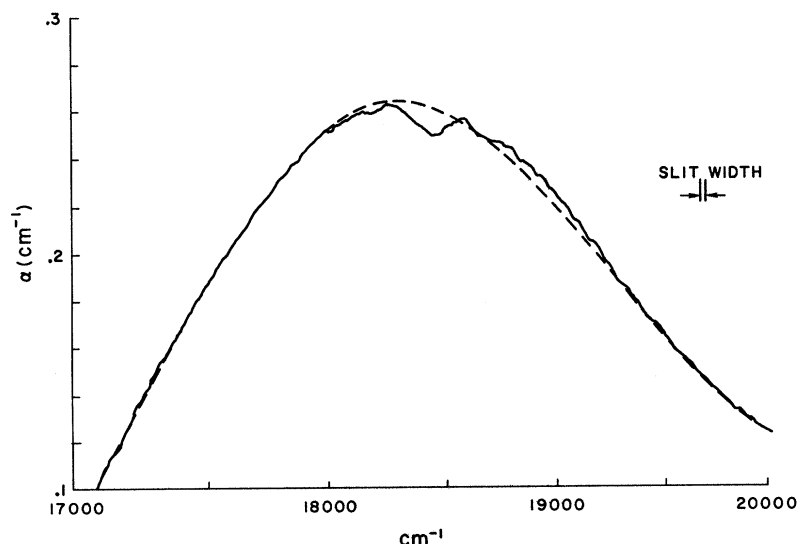


Fig. 4. Absorption spectrum of $KMgF_3: V^{2+}$ in the region of the $^4A_2 \rightarrow ^2T_2$ transition.

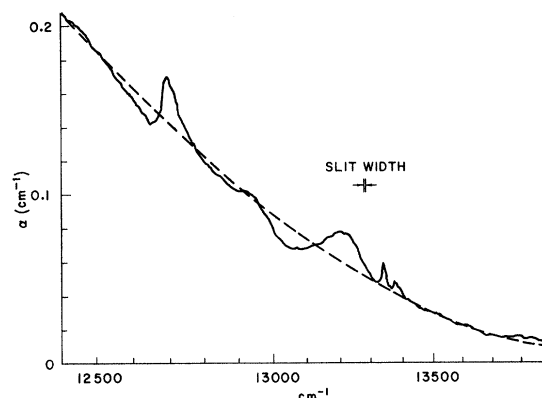


FIG. 3. Absorption spectrum of $KMgF_3: V^{2+}$ in the region of the $^4A_2 \rightarrow ^2E$ and 2T_1 transitions. The dashed line is Eq. (2).

where $p = (\omega - \omega_0)/\bar{\omega}$, and α_0 , S , ω_0 , and $\bar{\omega}$ are adjustable parameters. S is the mean number of phonons emitted in the transition, and $\hbar\bar{\omega}$ their mean energy. The fitted Pekarian is shown by the dashed line in Figs. 3 and 4.²¹ The effect of subtracting out α_B is shown in Figs. 5-7. In the case of the $^4A_2 \rightarrow ^2T_1$ transition, the background includes a contribution from the broad 2E vibronic centered near $13\,150\text{ cm}^{-1}$. We have estimated this as best we can to obtain the points in Fig. 7.

It is important that we be certain of the assignments of these transitions. In particular, we want to know if they are purely electronic, or involve the emission of a phonon. If the former, they must be magnetic dipole (MD) in a centrosymmetric crystal such as $KMgF_3$; if the latter, they will almost certainly be electric dipole (ED). In a uniaxial crys-

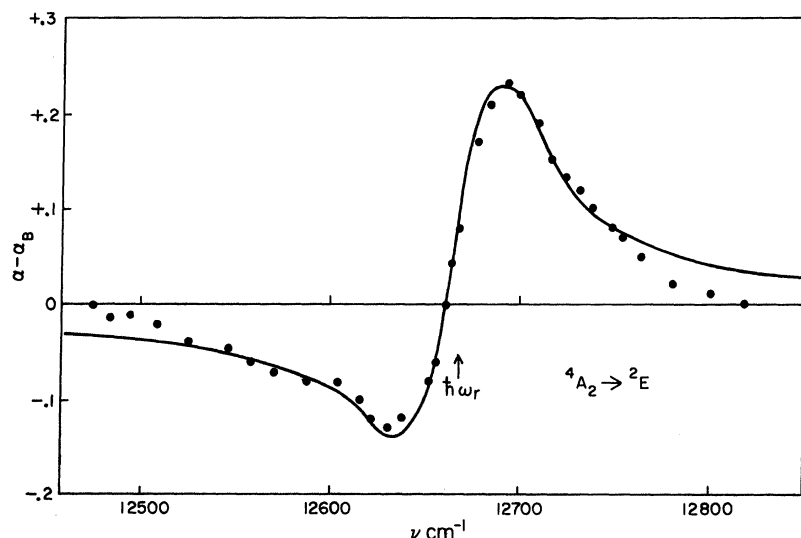


FIG. 5. ${}^4A_2 \rightarrow {}^2E$ transition of $\text{KMgF}_3:\text{V}^{2+}$, after subtraction of the background absorption. The full line is Eq. (1), with the parameters given in Table I.

tal, one can most easily determine the dipole character of a transition, if it is polarized, by comparing the π , σ , and α spectra.²² If the σ and α spectra agree, while π is different, the transition is ED; if π and α agree, while σ is different, it must be MD. This method is not available to us in KMgF_3 , which is cubic. We tried to induce polarization by stressing the crystal $\langle 001 \rangle$, but even at the breaking stress, the polarization of the absorption is too small to be detectable.

Instead, we turned to MgF_2 . This crystal is tetragonal, V^{2+} replacing Mg^{2+} in an octahedrally F^- coordinated centrosymmetric site, just as in KMgF_3 . (The fact that there are two Mg^{2+} sites, whose symmetry is orthorhombic, does not affect the argument concerning dipole character.) The spectrum of V^{2+} in MgF_2 is very similar to that in KMgF_3 , but the cubic terms are split by the orthorhombic field. In particular, the features which we associate with the ${}^4A_2 \rightarrow {}^2E$ and ${}^4A_2 \rightarrow {}^2T_2$ transitions are split and polarized. (We were unable to find

the weak ${}^4A_2 \rightarrow {}^2T_1$ transition in MgF_2 .) The spectrum in the range 7500–8000 Å is shown for the three polarizations in Fig. 8. The 4T_2 -band absorption is predominantly ED in this region. The two sharp features at 12630 and 12800 cm^{-1} are MD. This fact confirms their assignment to the ${}^4A_2 \rightarrow {}^2E$ no-phonon transition, split by the orthorhombic crystal field. There is a weakly polarized feature at 12830 cm^{-1} whose dipole character we cannot determine for certain, though it appears to be ED, and strong ED features near 13050 and 13220 cm^{-1} . These three features must be vibronic transitions associated with ${}^4A_2 \rightarrow {}^2E$.

The spectrum of $\text{MgF}_2:\text{V}^{2+}$ in the region of the ${}^4A_2 \rightarrow {}^2T_2$ transition is shown in Fig. 9. In Fig. 10 we show the result of subtracting out the strongly polarized 4T_1 background (assumed to be the sum of two Pekarians). In this case, the sharp feature is clearly ED, like the background, and must be vibronic. This is what we expect, since the ${}^4A_2 \rightarrow {}^2T_2$ transition borrows its intensity primarily

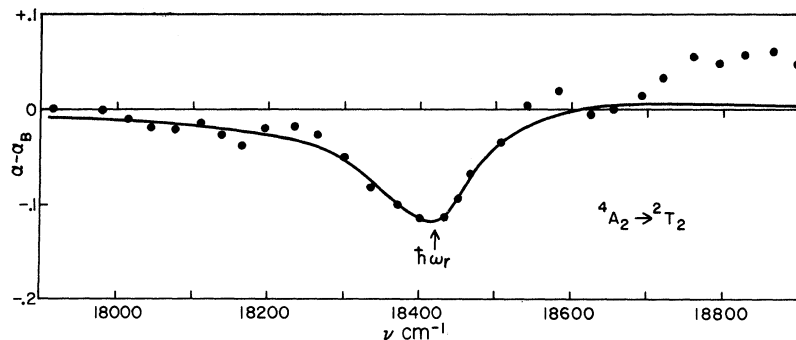


FIG. 6. Same as Fig. 5, for the ${}^4A_2 \rightarrow {}^2T_2$ transition.

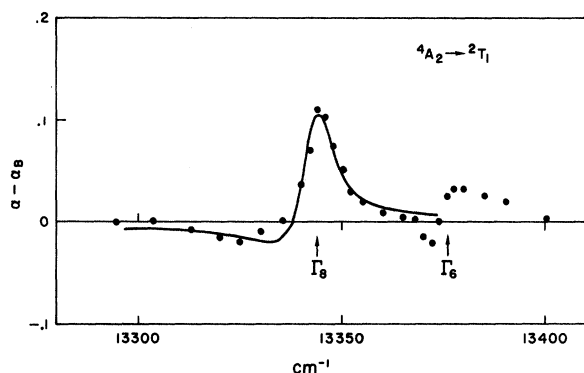


FIG. 7. Same as Fig. 5, for the ${}^4A_2 \rightarrow {}^2T_1$ transition.

from ${}^4A_2 \rightarrow {}^4T_1$, which is MD forbidden in O_h , so that the no-phonon line will be very weak.

Having established the MD character of the ${}^4A_2 \rightarrow {}^2E$ transition and the ED (vibronic) character of the ${}^4A_2 \rightarrow {}^2T_2$ transition, we return our attention to KMgF_3 . The full lines in Figs. 5-7 are Eq. (1), with the values of the parameters ω_r , $p = \alpha_0/\alpha_B$, q , γ listed in Table I.

For 2E , the values of p and q are accurate to 30%, and γ to 20%. For 2T_2 , q is very uncertain; a slightly different choice of α_B can even change its sign (see Refs. 16 and 21). Furthermore, as we have seen, the structure here is associated with a vibronic transition (probably one relatively sharp transition amongst many broader ones), and Eq. (1) should be convoluted with an effective phonon density of states. This could produce asymmetry, as well as extra width and structure. Thus 80 cm^{-1} is an upper limit for γ , and all we can say about q

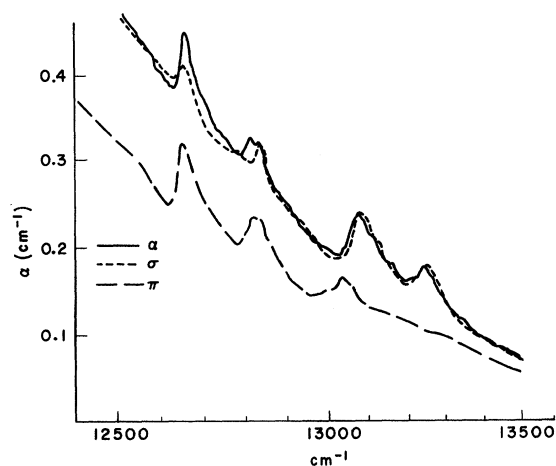


FIG. 8. Polarized absorption spectrum of $\text{MgF}_2:\text{V}^{2+}$ in the region of the ${}^4A_2 \rightarrow {}^2E$ transition.

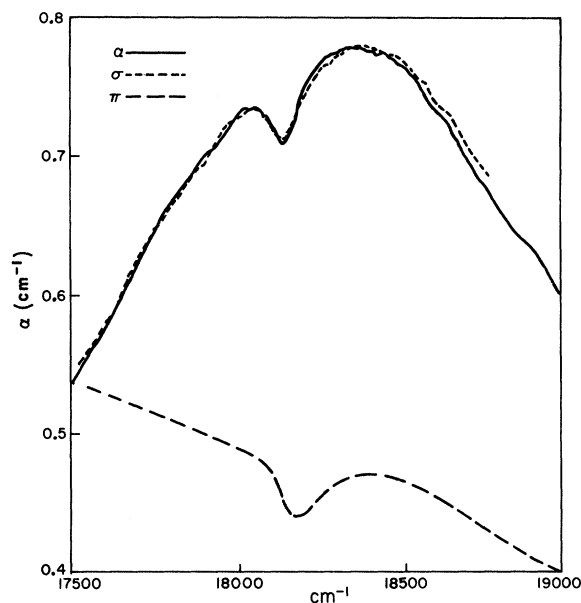


FIG. 9. Same as Fig. 8, for the ${}^4A_2 \rightarrow {}^2T_2$ transition.

is that it is small: $|q| \lesssim 0.5$.

In the case of 2T_1 , the uncertainty in background makes p and q uncertain. However, since so sharp a feature must be a no-phonon line, the value of γ is reliable (apart from an instrumental contribution of about 1.5 cm^{-1}), and the asymmetry of the line is genuine, indicating that q is positive and in the range 1.5-4.

The orthorhombic splitting of the electronic states in MgF_2 complicates the theory, and the fact that the spectra associated with different sharp transitions overlap makes the experimental data difficult to interpret quantitatively. The parameters obtained by fitting Eq. (1) to the MgF_2 data are not significantly different from the corresponding figures for KMgF_3 , and we will not discuss them further.

III. THEORY

We will set up a model system which, though oversimplified, exhibits the more important features of the spectra described in Sec. II. We will show that the model leads to Fano's formula, which was found to fit the data well, plus some additional terms which we can plausibly argue are small. The model gives values for the parameters q and γ in Fano's formula which are in good agreement with experiment.

We assume that we have an isolated center with an excited state ψ_2 , which has the same equilibrium lattice configuration as the ground state ψ_0 , but has a different spin, so that transitions to it are forbidden. We assume that nearby there is a state

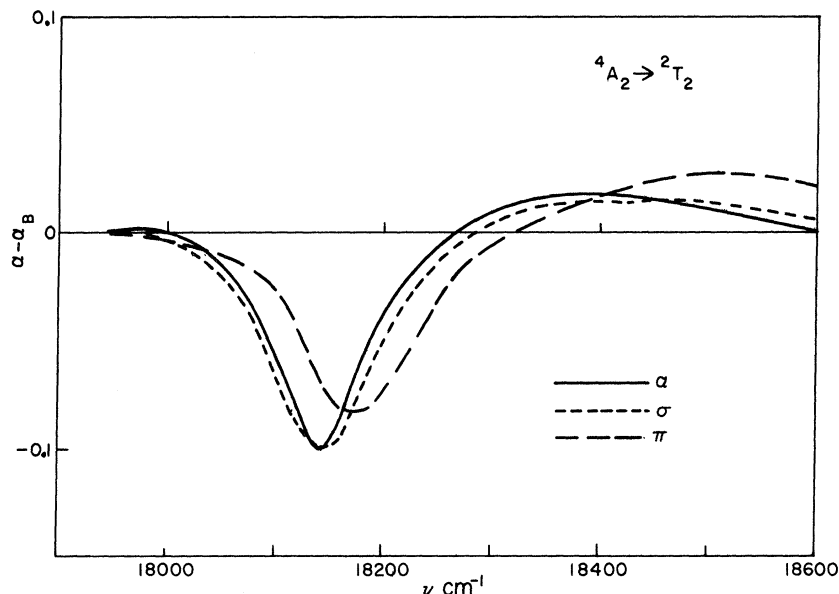


FIG. 10. Same as Fig. 9, after subtraction of the band absorption.

ψ_1 , to which MD transitions are allowed, and that ψ_1 and ψ_2 are connected by the spin-orbit coupling operator \mathcal{H}_{is} . We assume that the equilibrium lattice configuration for ψ_1 is displaced substantially from that of the ground state, so that the $\psi_0 \rightarrow \psi_1$ transition is broad relative both to \mathcal{H}_{is} and to the mean phonon frequency $\bar{\omega}$. This band overlaps the forbidden $\psi_0 \rightarrow \psi_2$ transition. For simplicity we assume that the force constants, and therefore the phonon frequencies, are independent of the electronic and vibrational state. Thus we have strong linear phonon coupling to the $\psi_0 \rightarrow \psi_1$ transition, and none (in the absence of spin-orbit mixing of ψ_1 and ψ_2) to the $\psi_0 \rightarrow \psi_2$ transition. The configuration-coordinate diagram for the problem is sketched in Fig. 11.

We ignore the extra complications introduced by the orbital degeneracy of ψ_1 and ψ_2 (Jahn-Teller effect), and assume that the basic vibronic states, before the application of spin-orbit coupling, are Born-Oppenheimer products $\psi_1\phi_m$ and $\psi_2\phi_n$. The electronic wave functions ψ are assumed to be in-

dependent of the phonon coordinates (Condon approximation). The transition dipole operator \mathbf{M} and the spin-orbit operator \mathcal{H}_{is} are also assumed to be independent of these coordinates.

For simplicity we assume that radiative decay

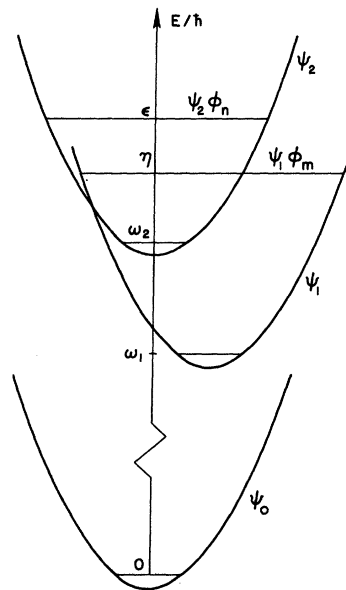


FIG. 11. Schematic configuration-coordinate diagram for V^{4+} in octahedral F^- coordination. The abscissa represents the mean radial displacement of the F^- ions (totally symmetric or Q_1 mode). Spin-orbit coupling is neglected.

TABLE I. Observed and calculated parameters in Eq. (1).

Transition	$\hbar \omega_r$	α_0/α_B	q		$\hbar \gamma$ (cm ⁻¹)	
⁴ A ₂ to:	cm ⁻¹	obs.	obs.	calc.	obs. ^a	calc. ^b
² E	12 670	0.08	+1.3	+1.0	25	33
² T ₁ (Γ ₈)	13 342	0.06	+2.3	+2.6	3.5	2.1
² T ₂	18 430	0.04	+0.2	+0.15	80	{ 50 (Γ ₇) 25 (Γ ₈)

^aIncludes a contribution of 1.5 cm⁻¹ (15 cm⁻¹ for 2T_2) from instrumental broadening.

^bAssuming $\xi = 150$ cm⁻¹.

can be neglected and that all measurements are made at 0°K.

A vibronic state associated with ψ_2 can be written as a Born-Oppenheimer product $|2\rangle|n\rangle$, where $|n\rangle = \Pi_\alpha |n_\alpha\rangle$, the product being taken over the $3N_0$ normal modes of the imperfect crystal. (N_0 is the number of atoms in the crystal.) The energy of this state (measured from the ground electronic state) is $\hbar\epsilon = \sum_\alpha n_\alpha \hbar\omega_\alpha + \hbar\omega_2$. Similarly a vibronic state associated with ψ_1 is written $|1\rangle|m\rangle$, where $m = \Pi_\alpha |m_\alpha\rangle$, and its energy is $\hbar\eta = \sum_\alpha m_\alpha \hbar\omega_\alpha + \hbar\omega_1$. Here $\hbar\omega_1$ and $\hbar\omega_2$ are the zero-phonon energy levels for ψ_1 and ψ_2 (see Fig. 11). Because of the displacement of the equilibrium lattice position associated with ψ_1 , states $|m_\alpha\rangle$ and $|n_\alpha\rangle$ are centered on different origins, so that

$$\varphi_{m_\alpha}(q_\alpha) = \varphi_{n_\alpha}(q_\alpha - a_\alpha)$$

when $m_\alpha = n_\alpha$. The displacement a_α of each oscillator is of order $N_0^{-1/2}$, but the sum $\frac{1}{2} \sum a_\alpha^2$ is finite, being the mean number of phonons emitted in the transition (conventionally called S , the Huang-Rhys parameter).^{19, 23, 24}

The matrix element for MD transitions from the ground state is $\langle 1 | \vec{M} \cdot \vec{H} | 0 \rangle \langle m | n = 0 \rangle$, which we abbreviate to $\hbar M H \langle m | 0 \rangle$. (M is isotropic in a cubic crystal.)

To clarify our method, we first consider the case of zero spin-orbit coupling. If we apply a weak oscillating field $2H \cos \omega t$, for a time short compared to the radiative lifetime of the excited states, the vibronic wave function $\Phi(t)$ is given by

$$\Phi(t) = |0\rangle|0\rangle + \sum_m y(m) |1\rangle|m\rangle. \quad (3)$$

The time-dependent Schrödinger's equation is

$$i\hbar \dot{\Phi}(t) = (\mathcal{H}_0 - \vec{M} \cdot \vec{H}) \Phi(t),$$

where

$$(\mathcal{H}_0 - \hbar\eta) |1\rangle|m\rangle = 0.$$

Integrating out $|1\rangle|m\rangle$, we have

$$i\dot{y}(m) = \eta y(m) - M \langle m | 0 \rangle \times 2H \cos \omega t, \\ y(m) = M \langle m | 0 \rangle \left(\frac{-He^{-i\omega t}}{\omega - \eta} + \frac{He^{i\omega t}}{\omega + \eta} \right).$$

The expectation value of the MD moment is

$$\langle M \rangle = \sum_m [M \langle 0 | m \rangle y(m) + M^* \langle m | 0 \rangle y^*(m)],$$

so that the complex susceptibility is

$$\chi(\omega) = N \langle M \rangle / 2H \cos \omega t = \hbar M^2 [G(\omega) + G(-\omega)], \quad (4a)$$

where

$$G(\omega) = G_1(\omega) + iG_2(\omega) = \sum_m \frac{|\langle 0 | m \rangle|^2}{\omega - \eta} \quad (4b)$$

and N is the number of impurity ions per unit volume. The nonresonant term $G(-\omega)$ is negligible and will be dropped. We could have achieved the same result by dropping all "negative frequency" ($e^{i\omega t}$) terms from the beginning. The imaginary part of the susceptibility χ_2 is proportional to the absorption constant, so that the absorption profile is given by

$$G_2(\omega) = \pi \sum_m |\langle 0 | m \rangle|^2 \delta(\omega - \eta), \quad (5a)$$

where

$$\int_{-\infty}^{\infty} G_2(\omega) d\omega = \pi. \quad (5b)$$

$G(\omega)$ could in principle be calculated, given some model for the phonons and for their interaction with the center. We prefer to regard $G_2(\omega)$ as an experimental quantity to be determined from the observed band profile, and to obtain $G_1(\omega)$ by the Hilbert transformation

$$G_1(\omega) = \pi^{-1} P \int_{-\infty}^{\infty} \frac{G_2(\omega') d\omega'}{\omega - \omega'}, \quad (6)$$

where P denotes the Cauchy principal value of the integral.

If we include spin-orbit coupling, states associated with ψ_2 become populated. The wave function is now given by

$$\Phi(t) = |0\rangle|0\rangle + \sum_m y(m) |1\rangle|m\rangle + \sum_n x(n) |2\rangle|n\rangle. \quad (7)$$

If we retain only terms in $e^{-i\omega t}$, the x 's and y 's obey the coupled equations

$$\omega y(m) = \eta y(m) + \Lambda \sum_n \langle m | n \rangle x(n) - M H e^{-i\omega t} \langle m | 0 \rangle, \quad (8a)$$

$$\omega x(n) = \epsilon x(n) + \Lambda \sum_m \langle n | m \rangle y(m), \quad (8b)$$

where

$$\Lambda = \hbar^{-1} \langle 2 | \mathcal{H}_{is} | 1 \rangle.$$

Substituting for $y(m)$ in (8b), we have

$$(\omega - \epsilon) x(n) = \Lambda^2 \sum_m \sum_{n'} \frac{\langle n | m \rangle \langle m | n' \rangle}{\omega - \eta} x(n') \\ - M \Lambda H e^{-i\omega t} \sum_m \frac{\langle n | m \rangle \langle m | 0 \rangle}{\omega - \eta}. \quad (9a)$$

Let

$$\sum_m \frac{\langle n | m \rangle \langle m | n' \rangle}{\omega - \eta} = Y(n, \omega) \delta_{nn'} + h(n, n', \omega), \quad (9b)$$

where $h(n, n', \omega) = 0$ if $n = n'$.

It is shown in the Appendix that

$$Y(n, \omega) = G(\omega - \epsilon + \omega_2), \quad (10)$$

where $G(\omega)$ is given by (4b), and that $h(n, n', \omega)$ is small over the energy range of interest if $G(\omega)$ is a slowly varying function of ω .

Then (9a) can be written

$$x(n) = [\omega - \epsilon - \Lambda^2 G(\omega - \epsilon + \omega_2)]^{-1} [-M\Lambda H e^{-i\omega t} G(\omega) \delta_{0n} - M\Lambda h(0, n, \omega) + \Lambda^2 \sum_{n'} h(n, n', \omega) x(n')]. \quad (11)$$

The first term in the numerator of (11) is dominant; that is, the contribution of the zero-phonon state of $|2\rangle$ is much larger than any other. This is what we might have expected from our assumption that the $\psi_0 \rightarrow \psi_2$ transition is not coupled to the lattice in the absence of spin-orbit coupling.

Substituting (11) and (8a) in (4a), we find for the complex susceptibility

$$\begin{aligned} \chi_1 + i\chi_2 = & -\hbar NM^2 \left(G(\omega) + \frac{\Lambda^2 [G(\omega)]^2}{\omega - \omega_2 - \Lambda^2 G(\omega)} \right. \\ & + \Lambda^2 \sum_n \frac{[h(0, n, \omega)]^2}{\omega - \omega_2 - \Lambda^2 G(\omega - \epsilon + \omega_2)} \\ & \left. - \frac{\Lambda^3}{MH} \sum_n \sum_{n'} \frac{h(0, n, \omega) h(n, n', \omega)}{\omega - \epsilon - \Lambda^2 G(\omega - \epsilon + \omega_2)} x(n') \right). \end{aligned} \quad (12)$$

The first term in (12) represents the $\psi_0 \rightarrow \psi_1$ band shape as it would be if there were no spin-orbit coupling. The second represents the perturbation of the band shape caused by coupling to the zero-phonon state of ψ_2 . It is resonant at $\omega = \omega_r = \omega_2 + \delta\omega$, where $\delta\omega = \Lambda^2 G_1(\omega_2)$. This is the (relatively small) shift in the energy of ψ_2 due to the interaction. The third and fourth terms are sums of terms resonant over a range of frequencies; they represent the contribution of vibronic states associated with ψ_2 . Since the density of such states is small for small ϵ , as are h (see Appendix) and $x(n)$, $n \neq 0$ [see Eq. (11)], their contribution in the interesting region near $\omega = \omega_2$ can be neglected. We then have for the susceptibility (whose imaginary part is proportional to the absorption coefficient)²⁵

$$\chi_1 + i\chi_2 = \hbar NM^2 \left(G(\omega) + \Lambda^2 \frac{(G_1 + iG_2)^2}{\omega - \omega_2 - \Lambda^2 G_1 - i\Lambda^2 G_2} \right). \quad (13)$$

Normalizing to the band absorption, and assuming it to vary only slowly near $\omega = \omega_r$, we have

$$-\chi_2/\hbar NM^2 G_2(\omega_r) = 1 + F(q, \xi), \quad (14a)$$

where

$$F(q, \xi) = (q^2 + 2\xi q - 1)/(1 + \xi^2),$$

$$\xi = [\omega - \omega_2 - \Lambda^2 G_1(\omega_2)/\gamma], \quad (14b)$$

$$\gamma = \Lambda^2 G_2(\omega_2), \quad q = G_1(\omega_2)/G_2(\omega_2).$$

Equations (14) have the same form as Fano's formula (1) for a sharp atomic transition overlapped by a continuum. Note that q is related to the ratio of the transition-dipole matrix elements for the sharp and broad states as modified by the interaction. In our case $\langle 2 | \underline{M} | 0 \rangle = 0$, and q is only nonzero because ψ_1 is mixed into ψ_2 by the spin-orbit interaction. This admixture would be zero if $G_1(0) = 0$, as would be the case, for instance, if $G_2(\omega) = \text{const}$.

There are some further complications to be considered before (14a) can be compared with experiment. When $\xi = -q$, (14a) gives $\chi_2 = 0$, contrary to the experimental observation that the minimum absorption is only a few percent below the band. The reason for this discrepancy is clear: only a small fraction of the band states takes part in the interference process. The bulk of the band absorption involves ED phonon-assisted transitions in which the final vibronic state has odd parity. Our calculation is limited to even-parity vibrations, since we assumed the transition moment to be independent of the phonon coordinates. Hence, only the MD part of the band is involved in the resonance near ω_r . [Interference between ED transitions will be considered later. It gives a nonresonant effect similar to, though larger than, the effect of the h terms in Eq. (12).] The integrated absorption of the ${}^4A_2 \rightarrow {}^4T_2$ band in $\text{KMgF}_3:\text{V}^{2+}$ is an order of magnitude greater than calculated for MD transitions,¹⁷ so we expect only about 10% of this band to be involved in the interference.

A further reduction occurs because not all the electronic states are connected by \mathcal{H}_{1s} . A 4T_2 or 4T_1 term contains a Γ_6 , a Γ_7 , and two Γ_8 levels. We can choose a linear combination of the two quartet Γ_8 's such that only one is coupled to the doublet level.²⁶ Thus for a Γ_8 state only one-third (on average) of the MD part of the band is involved in the interference. For a Γ_6 or Γ_7 state, this fraction is one-sixth.

Thus, in general, we expect to find, instead of (14a),

$$-\chi_2/\hbar NM^2 G_2 = 1 + pF(q, \xi), \quad (15)$$

where p is a number of order 0.03 which is difficult to estimate precisely.

The physical interpretation of γ is the same as

in Fano's theory; $2\hbar\gamma$ is the width of the sharp state ψ_2 , and $\frac{1}{2}\gamma^{-1}$ is the lifetime of ψ_2 against decay to ψ_1 . If there is any other decay process it must be convoluted with (15) to give the experimental profile. If we assume that the sum of all decay processes (other than interference with the band) produces a Lorentzian broadening of width $2\gamma'$, we find for the convoluted profile

$$-\chi_2/\hbar NM^2 G_2 = 1 + p (\xi'/\xi) F(q, \xi'), \quad (16)$$

where

$$\xi'/\xi = \gamma/(\gamma + \gamma').$$

Thus, an experimental profile may still have the Fano form even when it is substantially broadened by "unwanted" decay processes. The tendency of such processes, as one might expect, is to increase γ and to decrease p .

The effect of odd-parity vibrations, which induce ED transitions, can be included formally as follows. We take as normal modes linear combinations of phonons which have even or odd parity with respect to the impurity center. We write our Born-Oppenheimer basis states as $\psi\varphi\theta$, where φ refers (as before) to even-parity modes, and θ to the odd ones. The electronic part ψ now contains an odd-parity component which depends parametrically on θ . ED transitions can be induced by the excitation of one odd-parity mode; let the frequency of such a mode be ω_β . One possible vibrational wave function is

$$\theta_1(\beta) = \prod_{\alpha} |n_{\alpha}\rangle,$$

where $n_{\alpha} = 0$ for $\alpha \neq \beta$, and $n_{\beta} = 1$. The product is taken over all odd-parity modes which can induce a transition. Since \mathcal{H}_{is} is a purely electronic even-parity operator, states of different β are not coupled, and we can write a pair of equations, analogous to (7) and (8), for each β . Making the same approximations as for the MD case, we find for the contribution of the β mode to the susceptibility

$$\chi_{\beta}(\omega) = -\hbar NP_{\beta}^2 \left(G(\omega - \omega_{\beta}) + \frac{\Lambda^2 G(\omega - \omega_{\beta})}{\omega - \omega_2 - \omega_{\beta} - \Lambda^2 G(\omega - \omega_{\beta})} \right), \quad (17)$$

where²⁷

$$P_{\beta} = \hbar^{-1} \langle 1, n_{\beta} = 1 | \underline{P} | 0, n_{\beta} = 0 \rangle.$$

The ED contribution to the susceptibility is then $\sum \chi_{\beta}$. While (17) has the same form as (13), the sum is a convolution of (17) with the effective density-of-states function for the odd-parity modes (that

is, the true density of states weighted by the factor P_{β}^2). If this function could be approximated by a Lorentzian of width γ' , we would expect (16) to apply, with $p \sim 0.3$, rather than 0.03, since the bulk of the band is ED in character.

Note that only in a centrosymmetric system can we make a clearcut division into even- and odd-parity modes. In a system of sufficiently low symmetry, ED and MD transitions can interfere, at least in principle.

We conclude this section with a note on the adiabatic approximation. In the model on which we have based our calculations, the Born-Oppenheimer approximation is exact when $H_{is} = 0$. This is because we assume the electronic wave functions to be independent of the phonon coordinates q_{α} , and the correction term \mathcal{L} to the Born-Oppenheimer approximation then vanishes. (\mathcal{L} is called by Perlin²⁸ the "nonadiabaticity operator," and is defined by

$$\mathcal{L}(\psi\varphi) = \sum_{\alpha} \hbar\omega_{\alpha} \left(\frac{\partial\psi}{\partial q_{\alpha}} \frac{\partial\varphi}{\partial q_{\alpha}} + \frac{1}{2} \varphi \frac{\partial^2\psi}{\partial q_{\alpha}^2} \right), \quad (18)$$

where $\psi\varphi$ is a Born-Oppenheimer wave function.) When we include H_{is} , we can no longer write the wave function as a single product; it becomes a sum of products, with coefficients the x 's and y 's of Eq. (6).

An alternative approach, physically equivalent though mathematically much more complicated, would be to include H_{is} at an earlier stage, in the calculation of the Born-Oppenheimer products. For each value of the q 's we would solve the instantaneous electronic Hamiltonian, including H_{is} . The resulting electronic wave functions would now be functions of the q 's, and \mathcal{L} would no longer vanish. The off-diagonal elements of \mathcal{L} would mix the Born-Oppenheimer wave functions and in principle should give the same result as we obtained above. The calculation would be extremely complicated, however, since the potential curves on which the nuclei move would be very anharmonic where the spin-orbit interaction is strong. We only mention this alternative approach in order to stress the point that our calculation does take into account the essentially nonadiabatic nature of the problem.

IV. COMPARISON OF THEORY WITH EXPERIMENT

We must first consider whether our model is applicable to the $\text{KMgF}_3:\text{V}^{2+}$ system. We take our assumptions in turn.

(a) Does the "sharp" excited state (2E , 2T_1 , or 2T_2) have the same equilibrium lattice configuration as the ground (4A_2) state? In ruby the mean number of phonons emitted in the ${}^4A_2 \rightarrow {}^2E$ transition [the coupling parameter S in Eq. (2)] is of order 0.2 or less,²⁹ whereas it is of order 5 for the ${}^4A_2 \rightarrow {}^4T_2$ transition.³⁰ This difference is a consequence of

the fact that in the strong crystal-field limit the doublet states have the same electronic configuration (t_2^3) as the ground state, while 4T_2 has the (t_2^2e) configuration.³¹

In $\text{KMgF}_3\text{:V}^{2+}$ the cubic-crystal-field splitting Δ is somewhat smaller (relative to the interelectronic repulsion which mixes configurations), but our approximation $S=0$ should still be a reasonably good one for 2E and 2T_1 , and not too bad for 2T_2 .

(b) Can quadratic electron-lattice coupling and anharmonicity be neglected? The vibronic peaks associated with the ${}^4A_2 \rightarrow {}^4T_2$ transition are displaced from the no-phonon line by the same amount in absorption and emission.¹⁷ This shows that quadratic coupling is small near the no-phonon line. On the other hand, the 2E and 2T_1 resonances are some 2000 cm^{-1} above the ${}^4A_2 \rightarrow {}^4T_2$ no-phonon line, and absorption here is much stronger than the corresponding emission 2000 cm^{-1} below the no-phonon line. This is what one expects from anharmonicity (the equilibrium internuclear separation being greater in the excited state), but it could also indicate some quadratic coupling. By using the observed band absorption to calculate $G_2(\omega)$, we have, at least approximately, taken the quadratic interaction and anharmonicity into account. (To do so more precisely would be extremely difficult.) On the other hand, if the ED/MD ratio varies through the band, our assumed value of $G(\omega)$ for the MD transition could be somewhat in error.

(c) Can we neglect the orbital degeneracy of the band states? We know that one must take the Jahn-Teller effect into account in order to understand the spin-orbit structure of the ${}^4A_2 \rightarrow {}^4T_2$ no-phonon line.¹⁸ However, it was found that the Jahn-Teller coupling is primarily to E_g distortions, with a coupling parameter of order 1, compared with the over-all band value of order 5, which represents coupling primarily to A_{1g} distortions. Furthermore, since E_g distortions do not mix the 4T_2 states, the theory for them should be essentially the same as for the A_{1g} .

(d) While radiative decay can certainly be neglected, (the fluorescent lifetime of the 4T_2 states is 1.3 msec¹⁷), nonradiative transitions between doublets provide an alternative decay channel which may be important for the 2T_1 state.

(e) Is the mechanism for breaking the spin selection rule (which makes the "sharp" transition forbidden) spin-orbit coupling to the overlapping band? It can be seen from Fig. 2 of Ref. 32 that this is indeed the case for MD transitions to 2E and 2T_1 . Mechanisms not involving coupling to 4T_2 are weaker by a factor of order $(\Lambda/\Delta)^2$, and are hence, quite negligible. On the other hand, the ${}^4A_2 \rightarrow {}^4T_1$ transition is MD forbidden, and ${}^4A_2 \rightarrow {}^2T_2$ no-phonon transitions are only made possible by spin-orbit coupling of 2T_2 to 4T_2 and 4A_2 . Thus, there can be no inter-

ference between the no-phonon transition and the 4T_1 band. It was shown in Sec. II that the interference near 18 430 cm^{-1} is between ED transitions, and we have seen that we can obtain an antiresonant spectrum if the effective density of odd-parity phonon states is sufficiently sharply peaked (relative to γ).

We have already shown that (15) fits the experimental data for three transitions of V^{2+} in KMgF_3 , with the parameters given in Table I. Here we are concerned with comparing the fitted values of q and γ with theory. (As remarked above, it is difficult to predict p quantitatively. However, the estimated $p \sim 0.03$ for the 4T_2 band agrees with the observed values as well as can be expected.)

In estimating q and γ , we neglect broadening by alternative decay channels and assume that the MD part of the band has the same shape as the ED part, so that $G_2(\omega) = \pi \alpha(\omega) / \int \alpha(\omega) d\omega$. (In principle, we should allow for the displacement of the ED band by the mean frequency of the enabling vibrations, but in practice this is only a small correction.)

The Hilbert transform of G_2 , G_1 is found by numerical integration of (2). The results are shown in Figs. 12 and 13. We calculate Λ in terms of the one-electron spin-orbit coupling parameter $\xi' = (3/2)^{1/2} \langle t_2 \Gamma_8 | \mathcal{H}_{1s} | e \Gamma_8 \rangle$ by the method of Griffith,³³ obtaining the values of Λ/ξ' given in Table II. In Ref. 17 ξ' is found to be $150 \pm 10 \text{ cm}^{-1}$. Substituting G_1 , G_2 , and Λ in (14b), we obtain the calculated values of q and γ given in Table I. Agreement between calculated and observed values of q and γ is excellent, perhaps fortuitously so for the 2T_1 and 2T_2 resonances, in view of the uncertainties in the experimental data.

ACKNOWLEDGMENTS

One of us (M. D. S.) wishes to thank the Physics Department of the University of British Columbia for hospitality during the summer of 1969, and the National Research Council of Canada for partial support during this period. He is also grateful to R. C. Miller for comments on the manuscript, to K. A. Ingersoll for help with the experiments, and to K. L. Bhatia and R. Barrie for uncovering a mathematical error.

APPENDIX: EVALUATION OF THE SUM IN EQ. (9b)

We first consider the diagonal terms $Y(n, \omega) = \sum_m |\langle n | m \rangle|^2 / (\omega - \eta)$.

We follow the method which was used in Ref. 24 to calculate band shapes. We write

$$Y(n, \omega) = \sum_{m_\alpha} (\omega - \eta)^{-1} \prod_{\alpha} |\langle n_\alpha | m_\alpha \rangle|^2,$$

where α labels a phonon or resonance mode (true local modes are not considered). Consider the contribution to $Y(n, \omega)$ of all modes satisfying $\sum m_\alpha \omega_\alpha$

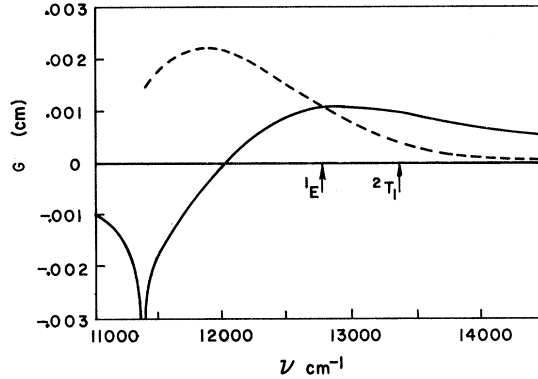


FIG. 12. Dashed line: Pekarian fit [Eq. (2)] to the ${}^4A_2 \rightarrow {}^4T_2$ absorption band of $\text{KMgF}_3:\text{V}^{2+}$, normalized to give $G_2(\omega)$. Full line: $G_1(\omega)$ obtained by numerical integration of Eq. (6).

$= \eta + \omega_1$. This contribution is $\sigma(n, \eta)/(\omega - \eta)$, where

$$\sigma(n, \eta) = \sum_{m_\alpha} \prod_{\alpha} |\langle n_\alpha | m_\alpha \rangle|^2 \delta\left(\eta + \omega_1 - \sum_{m_\alpha} m_\alpha \omega_\alpha\right).$$

We eliminate the δ function by taking the Fourier transform

$$\begin{aligned} \tilde{\sigma}(n, t) &= \int_{-\infty}^{\infty} e^{i\eta t} \sigma(n, \eta) d\eta \\ &= e^{-i\omega_1 t} \sum_{m_\alpha} \prod_{\alpha} |\langle n_\alpha | m_\alpha \rangle|^2 e^{im_\alpha \omega_\alpha t} \\ &= e^{i(\epsilon - \omega_1 - \omega_2)t} \sum_{m_\alpha} \prod_{\alpha} |\langle n_\alpha | m_\alpha \rangle|^2 e^{i(m_\alpha - n_\alpha)\omega_\alpha t}, \end{aligned}$$

since $\epsilon = \sum_{\alpha} n_\alpha \omega_\alpha + \omega_2$.

The sum product can be shown to be

$$\exp\left(-\sum_{\alpha} [n_\alpha a_\alpha^2 (1 - \cos \omega_\alpha t) + \frac{1}{2} a_\alpha^2 (1 - e^{-i\omega_\alpha t})]\right)$$

[Eq. (4.23) of Ref. 24], where a_α is the displacement ($\sim N_0^{-1/2}$) of the coordinate q_α . Only a few (a

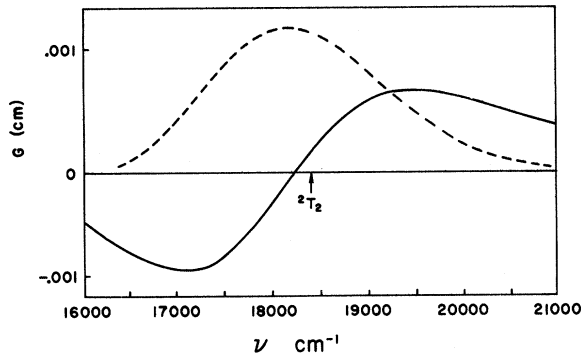


FIG. 13. Same as Fig. 12, for the ${}^4A_2 \rightarrow {}^4T_1$ band.

TABLE II. Spin-orbit matrix elements between some d^3 states.

$\hbar\Lambda = \langle {}^2\Gamma' \Gamma \mathcal{H}_{LS} {}^4\Gamma'' \Gamma \rangle,$ $ {}^4\Gamma'' \Gamma \rangle = \cos \varphi {}^4\Gamma'' \frac{3}{2} \Gamma_8 \rangle + \sin \varphi {}^4\Gamma'' \frac{5}{2} \Gamma_8 \rangle,$ $\xi' = (\frac{3}{2})^{1/2} \langle t_2 \Gamma_8 \mathcal{H}_{LS} e \Gamma_8 \rangle.$				
${}^2\Gamma'$	${}^4\Gamma''$	Γ	$\hbar\Lambda/\xi'$	$\tan \varphi^a$
2E	4T_2	Γ_8	$-2/\sqrt{3}$	3
2T_1	4T_2	Γ_6	$+1/\sqrt{2}$	
		Γ_8	$-1/2$	-2
2T_2	4T_1	Γ_7	$-(\frac{3}{2})^{1/2}$	
		Γ_8	$\sqrt{3}/2$	-2

^a The phase angle φ ($-\frac{1}{2}\pi < \varphi < \frac{1}{2}\pi$) is chosen so that $\langle {}^2\Gamma' | \mathcal{H}_{LS} | {}^4\Gamma'' \Gamma \rangle$, where $| {}^4\Gamma'' \Gamma \rangle = -\sin \varphi | {}^4\Gamma'' \frac{3}{2} \Gamma_8 \rangle + \cos \varphi | {}^4\Gamma'' \frac{5}{2} \Gamma_8 \rangle$. The wave functions $| \frac{3}{2} \Gamma_8 \rangle$ and $| \frac{5}{2} \Gamma_8 \rangle$ are given by Griffith [J. S. Griffith, *Theory of Transition Metal Ions* (Cambridge U. P., Cambridge, England, 1961), Table A20].

number of order $\epsilon/\bar{\omega}$ where $\bar{\omega}$ is the mean phonon frequency) of the $3N_0$ modes are excited; hence, the contribution of the first term is negligible. Hence,

$$\begin{aligned} \tilde{\sigma}(n, t) &= \exp[i(\epsilon - \omega_1 - \omega_2)t - \sum_{\alpha} \frac{1}{2} a_\alpha^2 (1 - e^{-i\omega_\alpha t})] \\ &= e^{i(\epsilon - \omega_2)t} \tilde{\sigma}(0, t). \end{aligned}$$

Transforming back into the frequency domain:

$$\begin{aligned} \sigma(n, \eta) &= \int_{-\infty}^{\infty} e^{-i(\eta - \epsilon + \omega_2)t} \tilde{\sigma}(0, t) dt \\ &= \sigma(0, \eta - \epsilon + \omega_2), \end{aligned}$$

$$\begin{aligned} Y(n, \omega) &= \sum_{\eta} \frac{\sigma(0, \eta - \epsilon + \omega_2)}{\omega - \eta} \\ &= G(\omega - \epsilon + \omega_2). \end{aligned}$$

Now let us turn to those off-diagonal terms in which $|n'\rangle$ only differs from $|n\rangle$ by the excitation of one mode, labeled β , so that $\epsilon' - \epsilon = \omega_\beta$. The state $|m\rangle$ may then have $m_\beta = n_\beta$ or $m_\beta = n'_\beta$. Taking the former case first, let

$$\begin{aligned} \sigma_+(n, n', \beta) &= \sum_{m_\alpha, m_\beta} \prod_{\alpha} |\langle m_\alpha | n_\alpha \rangle|^2 \langle m_\beta | n_\beta \rangle \\ &\quad \times \langle m_\beta | n'_\beta \rangle \delta(\eta + \omega_1 - \sum m_\alpha \omega_\alpha), \end{aligned}$$

with $m_\beta = n_\beta$, then

$$\begin{aligned} \tilde{\sigma}_+(n, n', t) &= e^{i(\epsilon - \omega_1 - \omega_2)t} \sum_{m_\alpha, m_\beta} \prod_{\alpha \neq \beta} |\langle m_\alpha | n_\alpha \rangle|^2 \\ &\quad \times \langle m_\beta | n_\beta \rangle \langle m_\beta | n'_\beta \rangle e^{i(m_\alpha - n_\alpha)\omega_\alpha t}. \end{aligned}$$

The vibrational wave functions are simple harmonic oscillator functions centered on $q_\alpha = 0$ and $q_\alpha = a_\alpha$, respectively, and the overlap integrals are easily calculated to be²⁴

$$\begin{aligned}\langle m_\beta | n_\beta \rangle &= 1 - \frac{1}{2}(m_\beta + 1)a_\beta^2, \quad n_\beta = m_\beta \\ &= [\frac{1}{2}(m_\beta + 1)]^{1/2} a_\beta, \quad n_\beta = m_\beta + 1 \\ &= -(m_\beta/2)^{1/2} a_\beta, \quad n_\beta = m_\beta - 1.\end{aligned}$$

The probability of double excitation of a given mode is negligible, as is the term a_β^2 ; so that

$$\tilde{\sigma}_+(n, n', t) = 2^{-1/2} \tilde{\sigma}(n, t) \sum_\beta a_\beta.$$

The second case ($m_\beta = n_\beta$) gives

$$\tilde{\sigma}_-(n, n', t) = 2^{-1/2} \tilde{\sigma}(n', t) \sum_\beta a_\beta.$$

The one-phonon contribution to the off-diagonal term is thus

$$\begin{aligned}h_1(n, n', \omega) &= 2^{-1/2} \sum_\beta a_\beta \left[\sum_\eta \frac{\sigma(n, \eta)}{\omega - \eta} - \sum_\eta \frac{\sigma(n', \eta)}{\omega - \eta} \right] \\ &= 2^{-1/2} \sum_\beta a_\beta [G(\omega - \epsilon) - G(\omega - \epsilon')].\end{aligned}$$

Since $G(\omega)$ is slowly varying, the term in square brackets is approximately $(\epsilon' - \epsilon) G'(\omega)$. Note that

we cannot sum over β at this point, since $a_\beta \sim N_0^{-1/2}$. However, in Eq. (12) for χ , h always appears quadratically, and the sum is over all β (not just those satisfying $\omega_\beta = \epsilon' - \epsilon$). Since $\sum_\beta a_\beta^2 = 2S$, h_1 is of order $S^{1/2} \bar{\omega} G'(\omega')$.

Two-phonon contributions to h can be calculated in similar manner, giving

$$\begin{aligned}h_2(n, n', \omega) &= [G(\omega) - G(\omega - \epsilon - \omega_\beta) \\ &\quad - G(\omega - \epsilon' + \omega_\beta) + G(\omega - \epsilon')] \frac{1}{2} \sum_{\beta, \gamma} a_\beta a_\gamma,\end{aligned}$$

with $\epsilon' - \epsilon = \omega_\beta + \omega_\gamma$. Thus h_2 is of order $S \bar{\omega}^2 G''(\omega)$. Since $G''/G' \sim G'/G \sim (S \bar{\omega})^{-1}$, the third term in (12) would be less than the second by a factor of order S^{-1} , even if all the phonons had the same frequency. The spread of phonon frequencies makes it much less important. The fourth term in (12) is of the same order as the third.

*Work at the University of British Columbia supported in part by the National Research Council of Canada.

[†]Visiting scientist at the University of British Columbia, Vancouver 8, B. C., Canada, June–August, 1969.

¹H. Beutler, Z. Physik **93**, 177 (1935).

²R. P. Madden and K. Codling, Phys. Rev. Letters **10**, 516 (1963); F. J. Comes and H. G. Sälzer, Z. Naturforsch. **19A**, 1230 (1964); J. D. Morrison, J. Chem. Phys. **40**, 2488 (1964); J. A. R. Sampson, J. Opt. Soc. Am. **54**, 420, 842 (1964); S. M. Silverman and E. N. Lassettre, J. Chem. Phys. **40**, 1265 (1964); J. W. McGowan, Science **167**, 1083 (1970).

³R. P. Madden and K. Codling, Astrophys. J. **141**, 364 (1965); U. Fano and J. W. Cooper, Phys. Rev. **137**, A1364 (1965).

⁴O. K. Rice, J. Chem. Phys. **1**, 375 (1933).

⁵U. Fano, Phys. Rev. **124**, 1866 (1961).

⁶G. Breit and E. P. Wigner, Phys. Rev. **49**, 519 (1936); J. M. Blatt and V. F. Weisskopf, *Theoretical Nuclear Physics* (Wiley, New York, 1952), Chap. 8.

⁷Y. Toyozawa, Progr. Theoret. Phys. (Kyoto) **20**, 53 (1958); J. Phys. Chem. Solids **25**, 59 (1964).

⁸J. J. Hopfield, J. Phys. Chem. Solids **22**, 63 (1961); L. P. Zverev, M. N. Noskov, and M. Ya. Shur, Fiz. Tverd. Tela **2**, 2643 (1960) [Soviet Phys. Solid State **2**, 2357 (1961)].

⁹J. C. Phillips, Phys. Rev. Letters **12**, 447 (1964); Phys. Rev. **136**, A1714 (1964); in *Advances in Solid State Physics*, edited by F. Seitz and D. Turnbull (Academic, New York, 1966), Vol. 18, p. 56.

¹⁰J. J. Hopfield, P. J. Dean, and D. G. Thomas, Phys. Rev. **158**, 748 (1967).

¹¹Y. Toyozawa, M. Inoue, T. Inui, M. Okazaki, and E. Hanamura, J. Phys. Soc. Japan **22**, 1337 (1967); M. Okazaki, M. Inoue, Y. Toyozawa, T. Inui, and E. Hanamura, *ibid.* **22**, 1349 (1967); A. Shibata and Y. Toyozawa, *ibid.* **25**, 335 (1968).

¹²D. L. Rousseau and S. P. S. Porto, Phys. Rev. Letters **20**, 1354 (1968).

¹³A. S. Barker, Jr., and J. J. Hopfield, Phys. Rev. **135**, A1732 (1964).

¹⁴R. A. Cowley, E. C. Svensson, and W. J. L. Buyers, Phys. Rev. Letters **23**, 525 (1969).

¹⁵J. G. Angus, B. J. Christ, and G. C. Morris, Australian J. Chem. **21**, 2153 (1968); J. Jortner and G. C. Morris, J. Chem. Phys. **51**, 3689 (1969).

¹⁶M. D. Sturge, J. Chem. Phys. **51**, 1254 (1969).

¹⁷M. D. Sturge, F. R. Merritt, L. F. Johnson, H. J. Guggenheim, and J. P. van der Ziel, J. Chem. Phys. (to be published).

¹⁸M. D. Sturge, Phys. Rev. B **1**, 1005 (1970).

¹⁹S. I. Pekar, Zh. Eksperim. i Teor. Fiz. **20**, 510 (1950); K. Huang and A. Rhys, Proc. Roy. Soc. (London) **A204**, 406 (1950).

²⁰J. J. Markham, Rev. Mod. Phys. **31**, 956 (1959).

²¹In Ref. 16 we fitted the bands to a distorted Gaussian obtained from the semiclassical approximation. Here we prefer to use the Pekarian, which has a sounder theoretical basis. Either formula can be made to fit the bands away from the fine structure equally well.

²²These conventional designations define the polarization as follows: $\pi = \vec{E} \parallel \vec{c}$, $\vec{H} \perp \vec{c}$; $\sigma = \vec{E} \perp \vec{c}$, $\vec{H} \parallel \vec{c}$; $\alpha = \vec{E} \perp \vec{c}$, $\vec{H} \perp \vec{c}$. Here \vec{E} and \vec{H} are the electric and magnetic vectors of the light, and \vec{c} is the optic axis.

²³For a more extended discussion of the meaning of a_α , see Ref. 24, whose formalism we follow.

²⁴M. H. L. Pryce, in *Phonons*, edited by R. W. H. Stevenson (Plenum, New York, 1966), Chap. 15.

²⁵If $G_2(\omega_r) = 0$ (i.e., the band does not overlap the sharp transition) $\chi_2(\omega_r)$ is apparently indeterminate. However, we must remember that the electromagnetic field is only applied for a finite time, so that ω is in fact complex, and should be replaced by $\omega + i\epsilon$. As $\epsilon \rightarrow 0$, we have $\chi_2(\omega) \rightarrow -\pi M^2 \Lambda^2 G_1^2 \delta(\omega - \omega_r)$, where $\pi \Lambda^2 G_1^2$ is the fraction of the band strength "borrowed" by the sharp spin-forbidden transition through the spin-orbit coupling.

²⁶We should really combine two degenerate vibronic

states $\psi_a\varphi_a$ and $\psi_b\varphi_b$, where ψ_a and ψ_b are Γ_8 states of 4T_2 or 4T_1 chosen to be diagonal in $3\mathcal{C}_4$. Since ψ_a and ψ_b have different energies, for exact degeneracy, $\varphi_a \neq \varphi_b$. We ignore this complication, which should not be important when $G_2(\omega)$ is slowly varying, and combine ψ_a and ψ_b to form ψ_1 before forming the Born-Oppenheimer product $\psi_1\varphi_1$.

²⁷Note that $P_B \sim N_0^{-1/2}$, where N_0 is the total number of ions in the crystal [see Ref. 24, Eq. (6.1)].

²⁸Yu. E. Perlin, Usp. Fiz. Nauk. **80**, 553 (1963) [Soviet Phys. Usp. **6**, 542 (1964)].

²⁹D. F. Nelson and M. D. Sturge, Phys. Rev. **137**, A1117 (1965).

³⁰D. S. McClure, J. Chem. Phys. **36**, 2757 (1962).

³¹Y. Tanabe and S. Sugano, J. Phys. Soc. Japan **9**, 766 (1954).

³²S. Sugano and Y. Tanabe, J. Phys. Soc. Japan **13**, 880 (1958).

³³J. S. Griffith, *Irreducible Tensor Method for Molecular Symmetry Groups* (Prentice-Hall, Englewood Cliffs, N. J., 1962). We have checked the relevant parts of his Table E1.

Self-Induced Transparency in Acoustic Paramagnetic Resonance

N. S. Shiren*

IBM, Thomas J. Watson Research Center, Yorktown Heights, New York 10598

(Received 24 February 1970)

Experiments on the propagation of microwave ultrasonic pulses through a resonant absorber are described. The principal features of self-induced transparency as described by McCall and Hahn for light pulses are observed. Quantitative measurements of pulse delay, output pulse width, energy, and area are in fair agreement with a calculation by Hopf which accounts approximately for the effect of the single reflection present in most of the experiments. Multiply reflected pulses exhibited linearly cumulative delay times, indicating constant reduced velocity during successive traversals through the absorber. Coherence-induced pulse breakup is shown to be a possible explanation of the pulse distortion and modulation observed in acoustic-paramagnetic-resonance experiments on Fe^{2+} .

I. INTRODUCTION

Several years ago the author reported that¹ the attenuation of microwave ultrasonic pulses by electron-spin-resonance transitions was accompanied by a large decrease in pulse velocity below the normal value in the host crystal. Velocity measurements were compared with small signal linear theories of signal velocity in a region of resonance absorption, as derived by Brillouin and by Baerwald.² Fair agreement was found if certain assumptions were made regarding the spatial distribution of the mechanism responsible for inhomogeneous broadening, and if it was also assumed that the transverse damping time of the spin system was shorter than the pulse width. While these observations utilized Ni^{2+} and Fe^{2+} impurities in MgO , the effect has also been observed by others on U^{4+} in CaF_2 .³

More recently, McCall and Hahn⁴ (MH) have derived a theory of electromagnetic pulse propagation including source terms, in Maxwell's equations, due to the coherently driven polarization of a two-level quantum-mechanical system. Under the condition that the pulse width is short compared with all damping time constants, pulses were found to propagate with greatly reduced velocities.

If one defines a pulse area

$$\theta(z) = (2p/\hbar) \int_{-\infty}^{\infty} \mathcal{E}(z, t) dt,$$

where p is the average electric dipole moment and $\mathcal{E}(z, t)$ is the electric field amplitude of a circularly polarized plane-wave pulse propagating along z , then θ is also the turning angle of dipoles at resonance. For input areas greater than a threshold value, $\theta = \pi$, MH find that after an initial reshaping and energy loss, steady-state pulses develop and no further energy loss occurs. They term this "self-induced transparency" (SIT).

Analytic solutions show that the steady-state pulses have areas $\theta = 2\pi n$ (n an integer), and for $n = 1$, the amplitude is

$$\mathcal{E}(z, t) = \frac{\hbar}{p\tau} \operatorname{sech}\left(\frac{t - z/V}{\tau}\right).$$

The pulse delay is given by

$$1/V - 1/c = \frac{1}{2} \alpha \tau \text{ sec/cm},$$

where c is the velocity in the nonresonant host, and the Beer's law energy absorption for very small-amplitude pulses is $e^{-\alpha z}$. Computer solutions carried out by Hopf and Scully⁵ confirm the theory of MH and also show that the pulse delays are even larger than above for input areas $\pi \leq \theta < 2\pi$.